Functional Materials 20, No.3 (2013)

Band structure of $LaPO_4$

S.V.Syrotyuk, Ya.M.Chornodolskyy*, V.V.Vistovskyy*, A.S.Voloshinovskii*, A.V.Gektin**

National University "Lviv Polytechnic",
12 S.Bandera St., 79013 Lviv, Ukraine
*I.Franko National University of Lviv,
8 Kyryla i Mefodiya St., 79005 Lviv, Ukraine
**Institute for Scintillation Materials, STC "Institute for Single Crystals",
National Academy of Sciences of Ukraine,
60 Lenin Ave.,61001 Kharkiv, Ukraine

Received March 11, 2013

The calculations of band structure of $LaPO_4$ crystal of monoclinic and hexagonal lattice symmetry is performed using the PAW formalism and taking into account the strong local correlations in the PBE0 GGA approximation. The obtained results are in good agreement with the experimental ones obtained from the luminescence excitation spectra of intrinsic emission of $LaPO_4$ crystal. The calculation of the partial electron state density of $LaPO_4$ crystal is performed and the nature of the various states in the overall density formation is explained.

Сделан расчет зонной структуры кристалла $LaPO_4$ для двух типов решеток — моноклинной и гексагональной, используя формализм PAW с учетом сильных локальных корреляций в приближении PBE0 GGA. Полученные результаты довольно хорошо согласуются с экспериментальными данными, определенными из спектров возбуждения собственной люминесценции кристалла $LaPO_4$. Произведен расчет парциальной электронной плотности состояний кристалла $LaPO_4$, объяснена природа различных состояний в формировании общей плотности.

Зонна структура $LaPO_4$. *С.В.Сиротюк, Я.М.Чорнодольський, В.В.Вістовський, А.С.Волошиновський, О.В.Гектін.*

Зроблено розрахунок зонної структури кристала $LaPO_4$ для двох типів граток — моноклінної і гексагональної, використовуючи формалізм PAW з урахуванням сильних локальних кореляцій у наближенні PBE0 GGA. Отримані результати добре узгоджуються з експериментальними даними, визначеними зі спектрів збудження власної люмінесценції кристала $LaPO_4$. Зроблено розрахунок парціальної електронної густини станів кристала $LaPO_4$, пояснено природу різних станів у формуванні загальної густини.

1. Introduction

$LaPO_4$ crystalline matrix is widely used for development of phosphors for fluorescent lamps, optical amplifiers, laser active mediums, etc. Process ability of this material and resistance for atmosphere influence caused the interest to study of the luminescent properties of $LaPO_4$ nanoparticles [1, 2]. $LaPO_4$ nanoparticles doped with rare earth elements attract attention because they can be used as luminescent biomarkers, nanoscintillators for radiotherapy or component of nanostructured composite scintillators.

In the process of interaction of high-energy electromagnetic radiation with nanoparticles the photoelectrons are produced. The mean free path of the photoelec-

trons is determined by the processes of electron-electron scattering. In the process of inelastic scattering of high-energy photoelectrons the secondary excitations are formed. For the secondary excitations a thermalization length is determined by processes of scattering on phonons. These parameters (free path length and thermalization length) are important for selection of the optimum nanoparticle size in the case of their use as nanoscintillators, especially, when these characteristics are commensurate with the nanoparticle sizes. Initial data for calculation of these parameters, such as an electron energy loss function and the effective masses of the charge carriers can be obtained from the analysis of the energy structure of crystals. This determines the relevance of the study of luminescent properties and electronic energy structure of $LaPO_4$.

It is known that nanoparticles $LaPO_4$ depending on their size can possess different symmetry of a lattice. The nanoparticles with a size up to ~20 nm have hexagonal, and the larger nanoparticles — monoclinic symmetry like their bulk analogues [3]. Only for the monoclinic lattice symmetry the calculations of the electronic energy structure for bulk $LaPO_4$ crystal was performed [4, 5]. Calculation of the electron energy in the $LaPO_4$ crystal for both structures (monoclinic and hexagonal) was performed in this work in the projector augmented waves (PAW) formalism taking into account the strong local correlations in the PBE0 GGA approximation [6].

2. Projector augmented waves method

The PAW method [7] combines features of pseudopotential and augmented plane waves methods. The wave $|\psi_n(\mathbf{r})\rangle$ and pseudowave $|\tilde{\psi}_n(\mathbf{r})\rangle$ functions are related:

$$|\psi_n(\mathbf{r})\rangle = \tag{1}$$
$$= |\tilde{\psi}_n(\mathbf{r})\rangle + \sum_a \sum_i (|\varphi_i^a(\mathbf{r})\rangle - |\tilde{\varphi}_i^a(\mathbf{r})\rangle)\langle \tilde{p}_i^a|\tilde{\psi}_n\rangle,$$

where $|\varphi_i^a(\mathbf{r})\rangle$ — atomic wave function, $|\tilde{\varphi}_i^a(\mathbf{r})\rangle$ — pseudowave function, $\langle \tilde{p}_i^a|$ — projector function.

Summation in (1) is performed on augmented spheres, which are numbered by index a. Index $i = \{n,l,m\}$ corresponds to the quantum numbers: the main, the orbital and the magnetic.

From equation (1) we see that

$$|\psi_n(\mathbf{r})\rangle = \tau|\tilde{\psi}_n(\mathbf{r})\rangle, \tag{2}$$

where the operator τ transforms pseudowave $|\tilde{\psi}_n(\mathbf{r})\rangle$ in the wave function $|\psi_n(\mathbf{r})\rangle$.

The explicit form of the operator τ follows from equation (1):

$$\tau = 1 + \sum_a \sum_i (|\varphi_i^a\rangle - |\tilde{\varphi}_i^a\rangle)\langle \tilde{p}_i^a|. \tag{3}$$

The stationary Schrodinger equation

$$H|\psi_{n\mathbf{k}}\rangle = |\psi_{n\mathbf{k}}\rangle\varepsilon_{n\mathbf{k}}, \tag{4}$$

with (2) gets the following view:

$$\tau^+ H\tau|\tilde{\psi}_{n\mathbf{k}}\rangle = \tau^+\tau|\tilde{\psi}_{n\mathbf{k}}\rangle\varepsilon_{n\mathbf{k}}, \tag{5}$$

where electron spectrum ε_n is same as in equation (4).

The electron density in the PAW method is defined by three terms [7]:

$$\rho(\mathbf{r}) = \tilde{\rho}(\mathbf{r}) + \sum_a (\rho^a(\mathbf{r}) - \tilde{\rho}^a(\mathbf{r})). \tag{6}$$

The first term — smooth pseudo density $\tilde{\rho}(\mathbf{r})$, which is represented by the Fourier transform

$$\tilde{\rho}(\mathbf{r}) = \sum_{n\mathbf{k}} f_{n\mathbf{k}}|\tilde{\psi}_{n\mathbf{k}}(\mathbf{r})|^2 = \frac{1}{\Omega}\sum_{\mathbf{G}}\tilde{\rho}(\mathbf{G})e^{i\mathbf{G}\mathbf{r}}, \tag{7}$$

where $f_{n\mathbf{k}}$ — occupation numbers of electron states, $\mathbf{k}$ — vector from the first Brillouin zone, n — number of zones populated by electrons, Ω — the unit cell volume, $\mathbf{G}$ — the reciprocal lattice vector.

For the function $\rho(\mathbf{r})$ formula (7) would look like this:

$$\rho(\mathbf{r}) = \sum_{n\mathbf{k}} f_{n\mathbf{k}}|\psi_{n\mathbf{k}}(\mathbf{r})|^2 = \frac{1}{\Omega}\sum_{\mathbf{G}}\rho(\mathbf{G})e^{i\mathbf{G}\mathbf{r}}. \tag{8}$$

There is a very significant difference between (7) and (8). It consist in the fact that the equation (7) requires the Fourier series expansion containing about ~10^3 vectors $\mathbf{G}$, whereas to achieve the same calculation accuracy using (8) it is needed ~10^6 ones. Therefore, it is impossible to solve the equation (4) using the function $|\psi_n(\mathbf{r})\rangle$ even on supercomputers.

The following two terms of electron density within the augmentation spheres are determined by projector coefficients of state occupation:

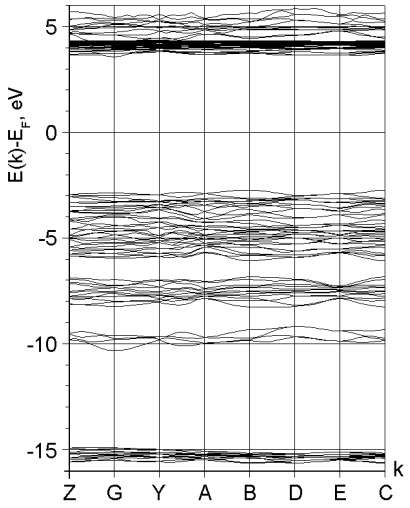

Fig. 1. The band structure of the $LaPO_4$ crystal possessing the monoclinic lattice symmetry.

$$W_{ij}^a \equiv \sum_{n\mathbf{k}} \langle \tilde{\psi}_{n\mathbf{k}} | \tilde{p}_i^a \rangle \langle \tilde{p}_i^a | \tilde{\psi}_{n\mathbf{k}} \rangle, \qquad (9)$$

that is:

$$\rho^a(r) = \sum_{ij} W_{ij}^a \varphi_i^{a^*}(r) \varphi_j^a(r), \qquad (10)$$

$$\tilde{\rho}^a(r) = \sum_{ij} W_{ij}^a \tilde{\varphi}_i^{a^*}(r) \tilde{\varphi}_j^a(r). \qquad (11)$$

The idea of PAW method is to transform the the Schrodinger equation to such an equation in which the unknown function of the state is $|\tilde{\psi}_{n\mathbf{k}}\rangle$. If one is found, then using τ (3) we can obtain the function of state $|\psi_{n\mathbf{k}}\rangle$. Using latter function the electron density and corresponding Hartree potential are obtained.

The exchange-correlation potential was chosen in the form of PBE0 [8–12], according to which the exchange-correlation energy is written as

$$E_{xc}^{PBE0}[\rho] = \\ = E_{xc}^{PBE}[\rho] + \frac{1}{4}(E_x^{HF}[\psi_{sel}] - E_x^{PBE}[\rho_{sel}], \qquad (12)$$

where PBE corresponds to the exchange-correlation functional [8], ψ_{sel} and ρ_{sel} — the wave function and the electron density of the selected electrons, respectively [12].

The exchange energy in the Hartree-Fock theory

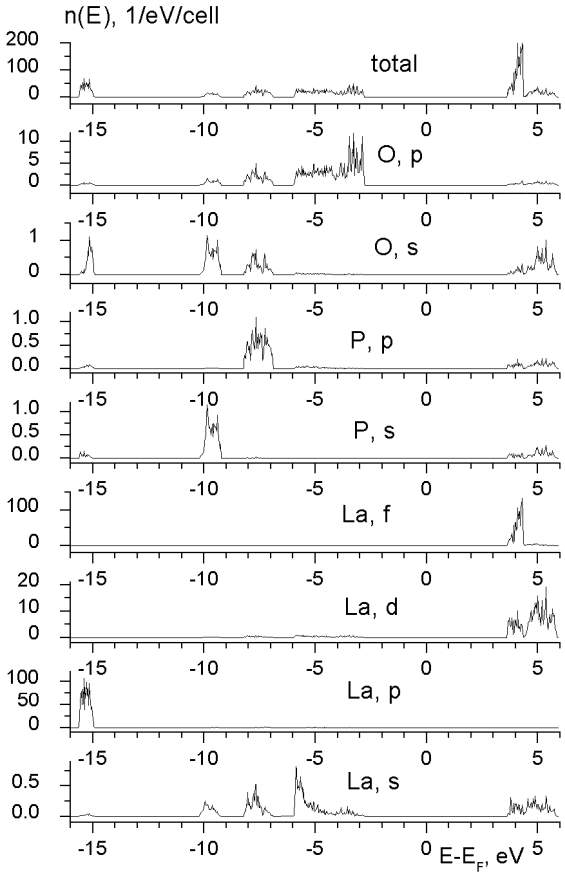

Fig. 2. The partial and total density of states of monoclinic $LaPO_4$ crystal. Partial density of states is shown in 1/ (eV·atom).

$$E_x^{HF}[\psi_{sel}] = \qquad (13)$$
$$= -\frac{1}{2}\sum_{nn'}^{occ} \delta_{\sigma_n,\sigma_{n'}} \int d\mathbf{r} d\mathbf{r}' \frac{\psi_n(\mathbf{r})\psi_{n'}^*(\mathbf{r})\psi_n^*(\mathbf{r}')\psi_{n'}(\mathbf{r}')}{|\mathbf{r}-\mathbf{r}'|},$$

where n, n' — quantum numbers of the occupied electron correlated states, σ_n and $\sigma_{n'}$ — corresponding spins. In the PAW method the calculation formula assumes the form [12, 13]:

$$E_x^{HF}[\psi_{sel}] = \qquad (14)$$
$$= -\frac{1}{2}\sum_{LM} \frac{4\pi}{2L+1} \sum_{d_i d_j d_k d_l} F^L_{d_i d_j d_k d_l} \sum_{m_i m_j m_k m_l} \langle m_i|LM|m_j\rangle \langle m_k|LM|m_l\rangle \sum_{\sigma} \rho_{ik}^{\sigma}\rho_{jl}^{\sigma},$$

where $\langle m_i\,|LM|\,m_j\rangle$ — Gaunt coefficients; $F^L_{d_i d_j d_k d_l}$ — Slater integrals [13], $\rho_{ij}^{\sigma} = \sum_{n\mathbf{k}} f_{n\mathbf{k}} \langle \tilde{\psi}_{n\mathbf{k}}^{\sigma} | \tilde{p}_i \rangle \langle \tilde{p}_j | \tilde{\psi}_{n\mathbf{k}}^{\sigma} \rangle$ — the electron density; coefficients $f_{n\mathbf{k}}$ — occupation num-

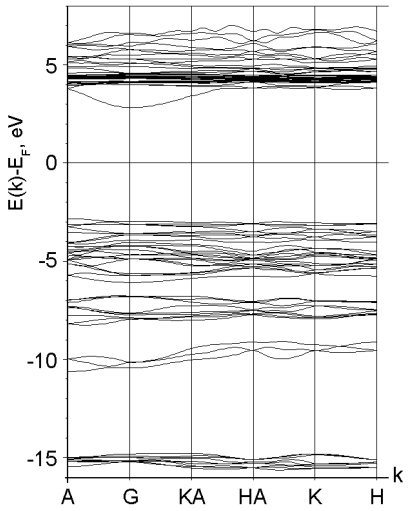

Fig. 3. The band structure of the $LaPO_4$ crystal possessing the hexagonal lattice symmetry.

bers of electron states. Index i of density ρ^{σ}_{ik} corresponds $i = \{d_i,\ m_i\}$, where $d_i = \{_i,\ n_i\}$ for selected d-orbitals.

For the calculation of the electronic energy structure of the $LaPO_4$ crystal pseudopotentials for the electronic configuration of the La $\{5s^25p^66s^25d^14f^0\}$, for P — $\{2s^22p^63s^23p^3\}$ and O — $\{2s^22p^4\}$ were generated using *atompaw* [14]. The treatment of enough deep electrons $\{5s^25p^6\}$ of La and $\{2s^22p^6\}$ of P as valence ones protects us from the ghost solutions (ghost states), which can be obtained in the case of minimal sets of valence basis functions [15]. The values of the augmentation spheres radii r_{PAW} were following: 2.4, 1.1 and 1.0 a.u. for La, P and O, respectively.

3. The calculation results and discussion

The electron energy spectrum of monoclinic $LaPO_4$ crystal is shown in Fig. 1. It can be seen that the spectrum of the crystal is characterized by an indirect gap G–B, which is 6.4 eV. The values of the direct interband gaps at different points of the Brillouin zone are following: 6.6 eV (Z), 6.5 eV (G), 6.7 eV (Z), 6.6 eV (A), 6.5 eV (B), 6.7 eV (D), 6.6 eV (E) and 6.5 eV (C). Fermi level chosen as reference energy is in the forbidden bandgap and it is almost equidistant from the top of valence band and the bottom of the conduction band.

Fig. 2 shows the total and partial density of states of monoclinic $LaPO_4$ crystal. As it follows from the figure the top of the valence band is formed predominantly by p states of oxygen with admixture of small

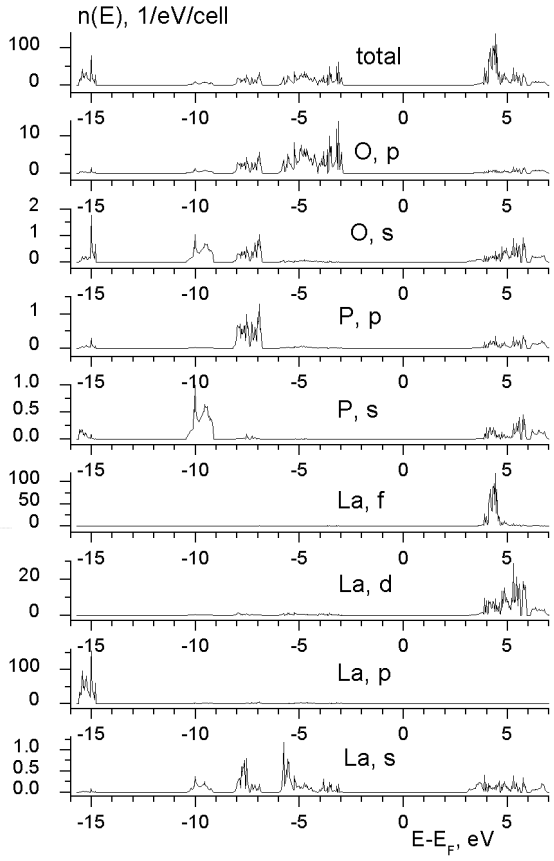

Fig. 4. The partial and total density of states of hexagonal $LaPO_4$ crystal. Partial density of states is shown in 1/ (eV·atom).

amounts of lanthanum s states. The bottom of the conduction band is created by hybridized d and f states of La with a small part of s states La and O as well as s and p states of P.

Fig. 3 shows the electronic band structure of the hexagonal $LaPO_4$ crystal. This crystal as well as its monoclinic modification (Fig. 1) is characterized by indirect forbidden bandgap G–A equal to 5.9 eV. The values of the direct interband gaps at various points of Brillouin zone are following: 6.6 eV (A), 6.0 eV (G), 6.4 eV (KA), 6.9 eV (HA), 6.9 eV (K) qand 6.9 eV (H). Fermi level, as well as for the monoclinic modification, is approximately in the middle of the forbidden bandgap.

The density of electron states for hexagonal $LaPO_4$ crystal is shown in Fig. 4. In this crystal the top of valence band is formed by hybridized s states of La and p states of O, too. In the vicinity of the bottom of conduction band the strongly hybridized d and f states of La dominates. Also the small part of s states of La and s states

of O together with *s* and *p* states of P are present there.

Comparison of the electron density of states of monoclinic (Fig. 2) and hexagonal (Fig. 4) $LaPO_4$ crystals shows that the maxima of the partial densities of *d* and *f* states of La and *s* states of O in the hexagonal crystal are located relatively Fermi level about 0.5 eV higher than in monoclinic crystal. This value agrees quite well with the experimental data: the forbidden bandgaps of monoclinic and hexagonal modifications of $LaPO_4$ nanoparticles defined by the empirical formula [16] using the spectral position of the exciton band in the excitation spectra of intrinsic luminescence at 10 K [17] are 8.6 and 8.0 eV, respectively.

4. Conclusions

The obtained results indicate that the forbidden bandgap of $LaPO_4$ crystal is 6.4 eV for monoclinic and is 5.9 eV for hexagonal modification. The difference of the forbidden bandgaps for the two lattice symmetries of $LaPO_4$ nanoparticles is in a good agreement with the experimental one determined from the excitation spectra of intrinsic luminescence of $LaPO_4$ crystal, where the decrease of the forbidden bandgap on about 0.6 eV is observed for hexagonal in comparison with monoclinic lattice symmetry.

Acknowledgement. This work is supported by 7th FP INCO.2010-6.1 grant agreement No.266531 (project acronym SUCCESS).

References

1. V.Pankratov, A.I.Popov, L.Shirmane et al., *J. Appl. Phys.*, **110**, 053522 (2011).
2. G.Stryganyuk, D.Trots, A.Voloshinovskii et al., *J. Luminescence*, **128**, 355 (2008).
3. A.V.Osipov, L.P.Mezentseva, I.A.Drozdova et al., *Glass Phys. Chem.*, **35**, 431 (2009).
4. K.C.Mishra, I.Osterloh, H.Anton et al., *J. Luminescence*, **72–74**, 144 (1997).
5. J.Wang, Y.Zhou, Zh.Lin, *Appl. Phys. Lett.*, **87**, 051902 (2005).
6. P.E.Blochl, *Phys. Rev. B*, **50**, 17953 (1994).
7. A.R.Tackett, N.A.W.Holzwarth, G.E.Matthews, *Computer Phys. Comm.*, **135**, 348 (2001).
8. J.P.Perdew, K.Burke, M.Ernzerhof, *Phys. Rev. Lett.*, **77**, 3865 (1996).
9. M.Ernzerhof, G.E.Scuseria, *J. Chem. Phys.*, **110**, 5029 (1999).
10. P.Novak, J.Kunes, L.Chaput, W.E.Pickett, *Phys. Stat. Sol. (b)*, **243**, 563 (2006).
11. E.Tran, P.Blaha, K.Schwarz, P.Novak, *Phys. Rev. B*, **74**, 155108 (2006).
12. F.Jollet, G.Jomard, B.Amadon et al., *Phys. Rev. B*, **80**, 235109 (2009).
13. X.Gonze, B.Amadon, P.-M.Anglade et al., *Computer Phys. Comm.*, **180**, 2582 (2009).
14. N.A.W.Holzwarth, A.R.Tackett, G.E.Matthews, *Computer Phys. Comm.*, **135**, 329 (2001).
15. N.A.W.Holzwarth, G.E.Matthes, R.B.Dunning et al., *Phys. Rev. B*, **55**, 2005 (1997).
16. A.H.Krumpel, A.J.J.Bos, A.Bessiere et al., *Phys. Rev. B*, **80**, 085103 (2009).
17. V.Vistovskyy, T.Malyi, A.Voloshinovskii et al., Hasylab Annual Report (2010). http://photon-science.desy.de/annual_report/files/2010/20101413.pdf.